Available online at www.sciencedirect.com

ScienceDirect

Procedia Structural Integrity 44 (2023) 1616–1623

Structural Integrity Procedia

www.elsevier.com/locate/procedia

XIX ANIDIS Conference, Seismic Engineering in Italy

Seismic reliability of RC frames casted with EAF concretes

Flora Faleschini*[a,b], Mariano Angelo Zanini[a], Klajdi Toska[a]

[a]*Dept. of Civil, Environmental and Architectural Engineering, University of Padua, Via Marzolo 9, Padua, 35131, Italy*
[b]*Dept. of Industrial Engineering, University of Padua, Via Gradenigo 6, 35131 Padua, Italy*

Abstract

The use of recycled aggregates is one way to fulfill sustainability goals in concrete industry, and among others, Electric Arc Furnace (EAF) slag aggregates has been proven to be promising. Past research demonstrated a significant increase of mechanical properties of EAF concretes when compared with ones made with natural aggregates (NA); however, at the same time, their use implies also an increase of self-weight loads. The present study aims therefore to investigate the seismic reliability of reinforced concrete frame buildings made with EAF, and compare it with the same structural configurations built with NA mixes, in order to show how the change in mechanical properties and self-weight can impact the seismic response of the analyzed case-studies.

Keywords: concrete; aggregates; EAF slag; seismic behavior; reliability

1. Introduction

Creating more sustainable materials to be implemented in the construction industry is a challenge the research community is trying to tackle with huge efforts. Among others, implementing electric arc furnace (EAF) slag as concrete aggregates in substitution to the natural ones has been proved to be promising technique to create more sustainable reinforced concrete (RC) structures.

EAF slag properties depend highly on steelmaking processes, which differ facility by facility, and from country to country. A consequence of such heterogeneity of this material is the current difficulty for the standardization of the EAF slag. For instance, the density of the EAF slag is a direct example of the differences between the slag properties among each steelmaking industry: Santamaria et al. (2017) have recorded it to be within a range of 3 to 4 Mg/m^3. This depends mainly on the content of metallic iron ($\rho \approx 8$ Mg/m^3), iron and manganese oxides ($\rho \approx 5$ Mg/m^3) and the

* Corresponding author. Tel.: +39 049 827 5585.
E-mail address: flora.faleschini@unipd.it

10.1016/j.prostr.2023.01.207

internal porosity. Santamaria et al. (2017) have also highlighted that, in spite of the different properties of the slag that can influence the properties of the final concrete, there are other factors that have higher influence in the mechanical properties of the concrete, and for these reason, this material results as a promising aggregate for concrete realization.

Studies in literature have shown that EAF slag use in concrete mixtures leads to positive enhancement of concrete mechanical properties (Pellegrino and Gaddo, 2009; Faleschini et al., 2015; Faleschini et al. 2017a; AbuEishah et al. 2012; Rondi et al., 2016). Typically, before its utilization, pre-treatment aimed at reducing potential expansion due to free CaO and MgO are necessary. When used in the coarse fraction, it allows achieving enhanced properties in terms of compressive and tensile strength gain and increased elastic modulus. Further, it improves durability, an thermal stability and residual properties after high temperature exposure, and even higher radiation attenuation (Arribas et al., 2014; Ortega-Lopez et al., 2018; Faleschini et al., 2019; Pomaro et al., 2019). Radiation attenuation is particularly due to EAF slag concrete higher specific weight, that can be estimated between 15-25% (Zanini et al., 2019). Concerning the use as fine aggregate, studies have shown that it does not allow to achieve the same benefit in terms of mechanical strength (Pellegrino et al., 2013; Santamaria et al., 2019). Recent experimental works have also demonstrated the feasibility of EAF concrete use in structural elements, leading to similar or in some cases even better structural behavior than in elements made with reference concrete. For instance, Pellegrino and Faleschini (2013) have tested reinforced concrete (RC) beams failing both in bending and shear, and in both cases improved load-carrying capacity was obtained by EAF concrete members. Faleschini et al. (2017b) investigated the behavior of RC exterior beam-column joints, subject to increasing cyclic load and constant axial force, obtaining higher ductility, dissipated energy and higher shear strength of the panel joint with respect to the reference test specimens. Lastly, Lee et al. (2018) tested RC columns under lateral and axial loading, demonstrating that the use of EAF concrete delayed the initiation of plastic hinges at the column ends, favoring the formation of plastic hinges at beam ends if employed in a RC frame, thus ensuring the formation of strong-column weak-beam mechanism.

The goal of the present research work is to investigate the influence of EAF concrete on the seismic behavior of RC structures. Four concrete materials were considered, a reference one made with natural aggregates and three EAF ones made with different substitution ratios. Three moment frame RC structures with three, six and nine stories, designed following the current Italian building codes (DM 17/01/2018), for a medium-to-high seismic hazard site were analyzed. Seismic fragility curves were computed from the seismic responses of the analyzed configurations under a set of non-linear time history analysis (NLTHAs) and a seismic reliability assessment was carried investigating the variation of structural safety margins related to the use EAF concrete mixtures in replacement to a conventional NA concrete.

2. Materials properties

EAF slags are dark stony materials deriving from the steelmaking industry. The presence of free lime and magnesium oxide in the initial composition makes EAF slag volumetrically instable, therefore, they are generally subjected to a weathering protocol in order to reduce slag expansion before employing them in a concrete matrix [35]. EAF slag are a high density, low porosity material characterized by a high crushing resistance. These characteristics positively influence the mechanical properties of concrete mixes where they are employed. the enhancement level depends on the amount of natural aggregate substitution and on the fraction of the slag used as substitute (beneficial effects is decreases when fine fraction is employed) [22]. Another important impact deriving from the use of slag aggregates regards the concrete specific weight. Depending on the slag composition the fresh and hardened concrete weight can increase between 15% and 20%.

In the present study four concrete mixes are considered. The first one is a standard concrete mix, with natural aggregates, to obtain a C25/30 class as defined by [EC2?]. The EAF concrete classes are defined based on a previous study from one of the authors [34] which analyzed 172 EAF concrete specimens from different experimental campaigns. Based on the mix properties, as w/c ratio, substitution ratio and slag fraction, three EAF concrete classes were proposed. The first class C1) collects 48 concrete samples with EAF coarse aggregates and w/c ratio $\leqslant 0.5$; the second class (C2) includes 38 specimens with coarse EAF aggregates and w/c ratio > 0.5. The last category contains 33 specimens with both fine and coarse EAF aggregates (A), and w/c ratio $\leqslant 0.6$. The dataset includes also 50 reference samples, which were used to evaluate strength and specific weight enhancement of EAF concrete compared to NA ones.

For each class, the mechanical characteristics can be obtained through simple coefficients that correlate the characteristics of the NA reference mix with the respective EAF concrete. The main mechanical characteristics for the four concrete material classes are reported in Table 1.

Table 1. Mechanical properties of the considered materials.

Aggregate type	Class	ρ_c [kN/m^3]	f_c [MPa]	f_{ct} [MPa]	E_c [MPa]
NA	C25/30	24.0	33.0	3.30	27000
	C1	28.0	46.0	4.22	35900
EAF	C2	28.0	46.3	3.63	29700
	A	27.7	30.2	3.56	28100

3. RC frames

Three RC frame structures with 3, 6 and 9 stories were considered in this study to evaluate their seismic behavior when built with standard and different EAF concrete mixtures (Table 1). The structures are characterized by a rectangular plan with five spans in the longitudinal direction and three in the transversal one, with equal column distance in both directions being 5 m and inter-story height of 3 m. The structures typical floor plan is shown in Figure 1a while in Figure 1b a 3D view of the 3-story building is reported. The structures were supposed to be located in a moderate-to-high seismic hazard site in Northeast Italy and designed in accordance with the current Italian Building Code considering a low ductility class (CD-B). Seismic forces were computed from a dynamic linear analysis while beams and columns were sized accordingly, using the reference C25/30 concrete strength class.

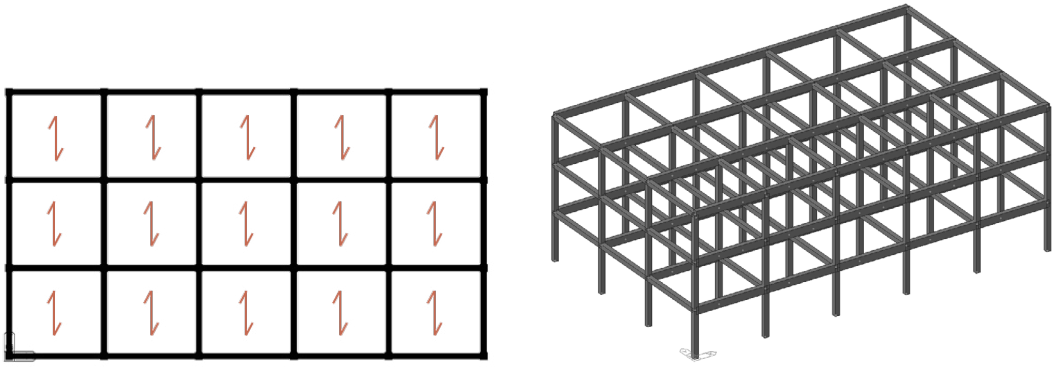

Figure 1: Floor layout of the RC structures a) and 3D view of the 3-story building case b).

4. Seismic reliability analysis

The occurrence of main shock events at a given site is assumed to be a Homogenous Poisson Process for the Performance-Based Earthquake Engineering (PBEE) framework (Cornell & Kravinkler.,2000). So, the process of events causing structural failure is also a HPP and its unique parameter, failure rate λ_f, can be used for computing the failure probability at any time. The failure rate depends on the seismicity of the site (hazard curve λ_{im}) and on the structural behavior (fragility curve $P[f|im]$). λ_f is computed by applying the Total Probability Theorem as:

$$\lambda_f = \int_{im} P[f|im] \cdot |d\lambda_{im}| \quad (1)$$

4.1. Seismic hazard analysis

The so-called Probabilistic Seismic Hazard Analysis for the computation of λ_{im} associates to each im value, the annual rate of events that exceed it at a given site. The seismicity of a given area di defined by three main components: the earthquake occurrence model, the spatial seismogenic model and the attenuation model. $|d\lambda_{\mathrm{im}}|$ represents the mean number of events per year with an intesity of exactly *im* and is obtained as:

$$|d\lambda_{\mathrm{im}}| = -\frac{d\lambda_{\mathrm{im}}}{d(im)}d(im) \tag{2}$$

On the other hand, λ_{im} is obtained via the following PSHA integral:

$$\lambda_{im} = \sum_{i=1}^{nSZ} \nu_{m_{min,i}} \int_{m_{min,i}}^{m_{max,i}} \int_{r_{min,i}}^{r_{max,i}} P[IM > im|m,r] f_{M_i}(m) f_{R_i}(r)\, dm\, dr \tag{3}$$

where $\nu_{m_{min,i}}$ is the rate of occurrence of earthquakes greater than a suitable minimum magnitude $m_{min,i}$ of the i^{th} seismogenic zone, $f_{M_i}(m)$ is the magnitude distribution for the i^{th} seismogenic zone and $f_{R_i}(r)$ is the distribution of the source i^{th}-to-site distance. Given a combination of magnitude *m* and distance *r*, $P[IM > im|m,r]$ is the probability to exceed im.

The seismic hazard map for Italy is provided by the National Institute of Geology and Volcanology (INGV). To compute the failure rate a continuous hazard function is needed. Since hazard data bu INGV (values of the 16th, 50th and 84th percentile) are provided only for nine return times, it is possible to fit the median values (i.e., the 50th percentile) with a quadratic function in the logarithmic space as:

$$\lambda(s) = k_0\, e^{(-k_1 \ln(s) - k_2 ln^2(s))} \tag{4}$$

In assessing seismic reliability, instead of the median hazard curve, it is more suitable to refer to the mean one which is possible to derive with the following equation:

$$\bar{\lambda}(s) = \lambda(s)\, e^{(\frac{1}{2}\beta_H^2)} \tag{5}$$

where β_H can be estimated as:

$$\beta_H = \frac{\ln(S_{84\%}) - \ln(S_{16\%})}{2} \tag{6}$$

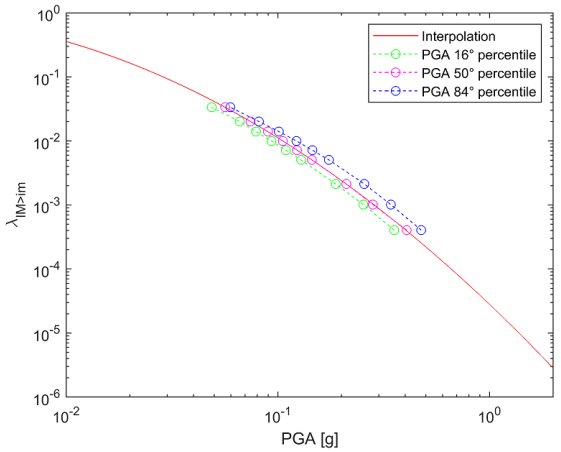

Figure 2: Interpolation of the seismic hazard curve in the considered site.

4.2. Seismic fragility analysis

The fragility function ($P[f|im]$) represents the probability to reach and exceed a certain damage state given a specific intensity im. Several frameworks for fragility function estimation exits in literature, the most popular ones are the Cloud Analysis [29], the Incremental Dynamic analysis [28] and the Multi-Stripes Analysis [30].

In this work the Cloud Analysis method is adopted. The fragility parameters are estimated starting from a set of n natural ground motion records. The fragility function is computed as follows:

$$[f|im] = P\left[EDP > \overline{edp}|im\right] = 1 - P\left[EDP \leq \overline{edp}|im\right] = 1 - \Phi\left[\frac{ln(\overline{edp}) - ln(edp)}{\beta}\right] \tag{7}$$

$\overline{edp}$ is the median threshold value of the assumed structural limit state, and edp represents the median estimate of the demand that can be computed with a ln-linear regression model, as:

$$ln(edp) = a + b \cdot ln(im) \tag{8}$$

β is the standard deviation of the demand conditioned on im and can be estimated from the regression of the seismic demands as:

$$\beta_H = \frac{\ln(S_{84\%}) - \ln(S_{16\%})}{2} \tag{9}$$

5. Results and discussion

To assess the seismic fragility of the considered structures a set of NLTHAs were carried out adopting a diffused plasticity model, using a fiber section discretization, to consider material non-linearities. Concrete behavior was modeled via the well-known Mander et al. (1988) model whereas the Menegotto and Pinto (1973) steel model was used for the non-linear behavior of rebars. Simulations were carried out via SeismoStruct software using a set of 30 natural ground motion records. All three components of the seismic wave were considered in the analysis. The Engineering Demand Parameter (EDP) parameter chosen for the fragility curve computation is the maximum inter-story drift ratio (IDR) while the peak ground acceleration (PGA) is used as Intensity Measure (IM). Four damage states: Slight, Moderate, Extensive and Complete, with corresponding EPD threshold of 0.4%, 0.8%, 1.5% and 3%, were defined. For the mid-rise and high-rise buildings, a reduction factor of respectively 2/3 and 1/2 as proposed by FEMA (2012) was considered to account for higher mode effects and differences between average computed in non-linear static analysis and maximum individual IDR from NLTHAs.

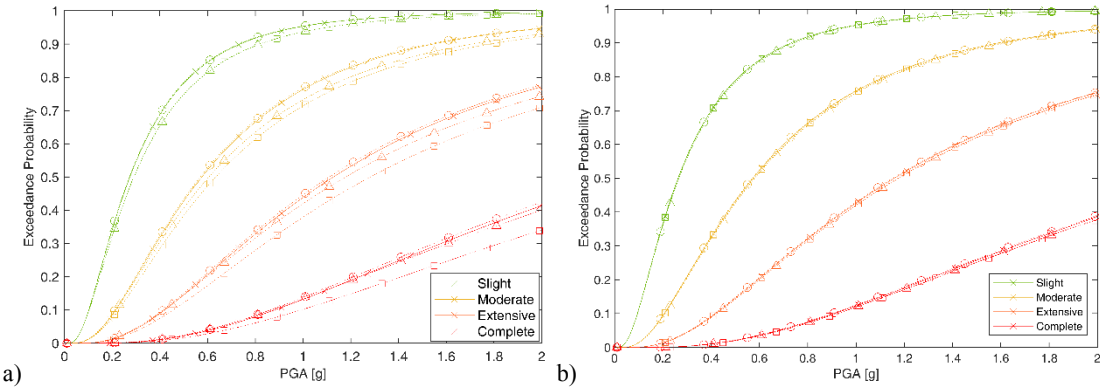

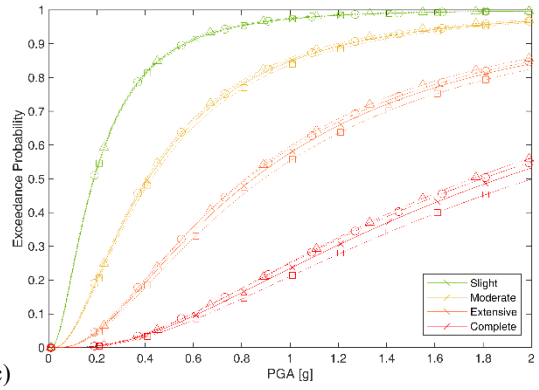

c)

Figure 3: Fragility curves for 3, 6 and 9 story buildings. Respectively: x – C25/30; triangle – C1, circle – C2 and square – A.

5.1. Seismic fragility

From the time histories registered building responses, fragility curves were built for each case, in accordance with the Cloud Analysis method. Figure 3 shows the fragility curves for the identified damage states (Slight, Moderate, Extensive and Complete). Additionally, x markers were used for frames realized with the reference concrete, triangle, circle and square ones were used for the classes of C1, C2 and A, respectively.

Results show how EAF concrete building performance to seismic solicitation is very similar to that of the buildings made with the reference material. For the 3- and 9-story buildings, the fragility curves tend to vary more while considering superior DSs, with the EAF-A material is less vulnerable to seismic actions. The 6-story building has almost an identical response for all the materials considered. In fact, the fragility curves are almost overlapping for all kind of materials used.

5.2. Seismic reliability

Mean failure rates were computed for each DS and RC structure considered and the results are summarized in Figure 4. When compared to the frames realized with the reference material, EAF concrete buildings report similar reliability indexes. This confirms that in terms of safety margins with respect to seismic actions, buildings designed with ordinary concrete but built with EAF aggregates are exposed to almost the same risk as those built with NAs ones. highlighting Such result leads us to derive the consequence that the partial or full replacement of NAs with EAF aggregates has a low impact in terms of seismic reliability levels, for the investigated structural systems subject to the analyzed range of seismic events. Mean failure rates are characterized by a decreasing trend of one order of magnitude moving from less severe to stronger DSs, with values in the order of 10^{-2} for Slight DS, 10^{-3} for Moderate DS, 10^{-4} for Extensive DS and 10^{-5} for Complete DS. Further, it can also be observed how mean failure fate values computed for the 9-story RC frame archetype are almost twice the ones derived for the 3- and 6- story archetypes, and this occurs regardless of the type of concrete. This fact underlies how it seems that the adoption of current code recommendations does not allow to design buildings characterized by the same level of seismic reliability, but some differences can be observed as herein shown, in particular comparing low-to-medium rise buildings with higher ones.

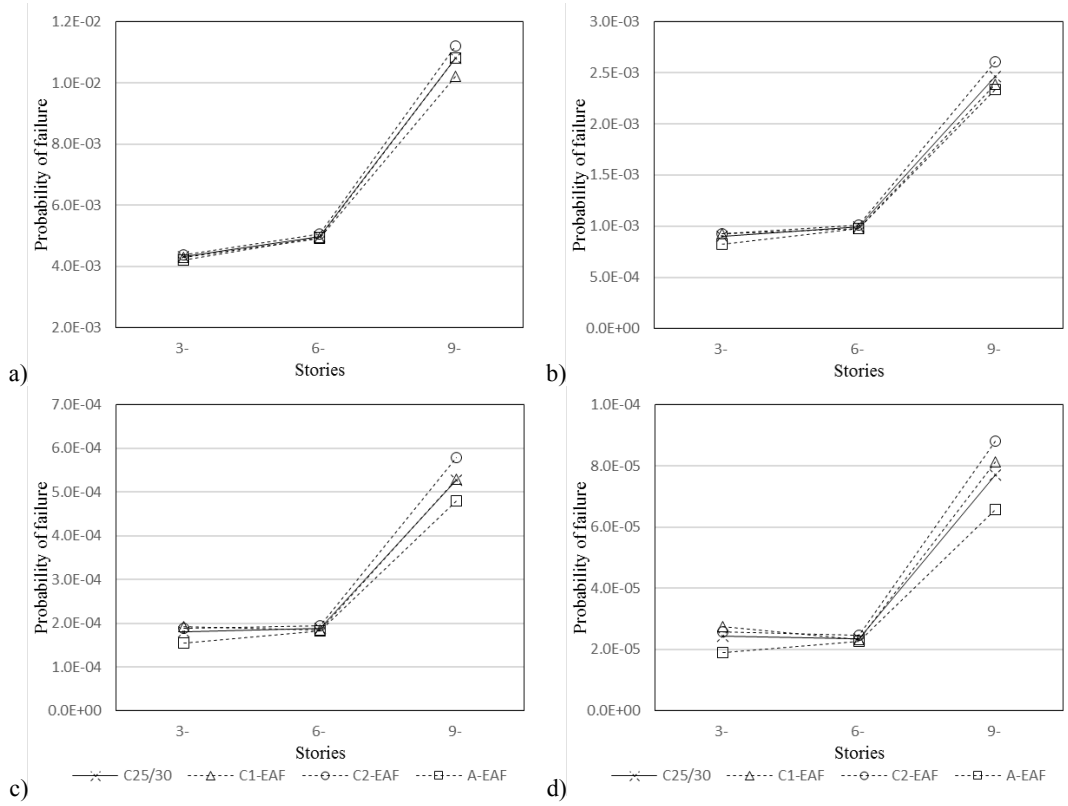

Figure 4: Probability of failure for a) slight, b) moderate, c) extensive and d) complete damage state.

4. Conclusion

The main goal of this research work was to investigate the effect of concrete mixtures with EAF slag as aggregates in substitution of natural ones, in the seismic performance of different code conforming RC-frame structures. The enhancement in terms of mass and stiffness due to the employment of EAF slag can lead to different seismic loads and global response of the structures. To analyze this effect fragility curves were computed through a set of NLTHAs taking into account also the variability of the material properties. Fragility functions and mean failure rates were computed for each combination of geometrical configuration and material and based on the results of the present study the following conclusions can be highlighted:

- Using materials that were proved to have higher mechanical strength might not improve the global seismic behavior of RC moment frame structures. The results analyzed here highlighted how partially replacing NAs with EAF aggregates has a low impact in terms of seismic reliability levels, for the analyzed cases.
- Seismic safety levels achieved by EAF RC building are comparable to those of the same structural configuration built with ordinary concrete.
- Higher mean failure rate was observed for the high-rise case (9- story) with respect to the low- and mid- rise ones. This marks out how current building codes may not ensure the same seismic reliability level for higher structures as for low- and mid- rise ones.

References

Abu-Eishah, S. I., El-Dieb, A. S., & Bedir, M. S. (2012). Performance of concrete mixtures made with electric arc furnace (EAF) steel slag aggregate produced in the Arabian Gulf region. Construction and Building Materials, 34, 249-256.

Arribas, I., Vegas, I., San-Jose, J. T., & Manso, J. M. (2014). Durability studies on steelmaking slag concretes. Materials & design, 63, 168-176.

Cornell C.A., Krawinkler H. (2000) Progress and challenges in seismic performance assessment. PEER Centre News, 3(2): 1-3.

DM 17/01/2018 (2018) Aggiornamento delle Norme Tecniche per le Costruzioni, Roma, Italy. (in Italian)

Faleschini, F., Fernández-Ruíz, M. A., Zanini, M. A., Brunelli, K., Pellegrino, C., & Hernández-Montes, E. (2015). High performance concrete with electric arc furnace slag as aggregate: mechanical and durability properties. Construction and Building Materials, 101, 113-121.

Faleschini, F., Hofer, L., Zanini, M. A., dalla Benetta, M., & Pellegrino, C. (2017a). Experimental behavior of beam-column joints made with EAF concrete under cyclic loading. Engineering structures, 139, 81-95.

Faleschini, F., Bragolusi, P., Zanini, M. A., Zampieri, P., & Pellegrino, C. (2017b). Experimental and numerical investigation on the cyclic behavior of RC beam column joints with EAF slag concrete. Engineering Structures, 152, 335-347.

Faleschini, F., Njinwoua, R., Beaucour, A.-L., Pliya, P., Noumowe, A., Pellegrino C. (2019). High-temperature behavior of heavy-weight concretes. International Conference on Sustainable Materials, Systems and Structures (SMSS 2019) Durability, Monitoring and Repair of Structures, 20-22 March 2019 – Rovinj, Croatia.

FEMA (2012) Earthquake Model, Hazus-MH 2.1 Technical Manual. Federal Emergency Management Agency, Washington DC, US (available at: www.fema.gov/plan/prevent/hazus).

INGV. Interactive Seismic Hazard Maps. Available at: http://esse1-gis.mi.ingv.it/s1_en.php (last access 04/03/2019).

Jalayer F., Cornell C.A. (2003). Direct probabilistic seismic analysis: implementing non-linear dynamic assessments. Stanford University, 2003.

Lee, J. M., Lee, Y. J., Jung, Y. J., Park, J. H., Lee, B. S., & Kim,

K. H. (2018). Ductile capacity of reinforced concrete columns with electric arc furnace oxidizing slag aggregate. Construction and Building Materials, 162, 781-793.

Mander J.B., Priestley M.J.N., Park R. (1988) Theoretical stressstrain model for confined concrete. Journal of Structural Engineering, 114(8): 1804-1826.

Menegotto, M., & Pinto, P. E. (1973). Method of analysis for cyclically loaded reinforced concrete plane force and bending. In Proceedings, IABSE Symposium on Resistance and Ultimate Deformability of Structures Acted on by Well Defined Repeated Loads, Lisbon (pp. 15-22).

Ortega-López, V., Fuente-Alonso, J. A., Santamaría, A., SanJosé, J. T., & Aragón, Á. (2018). Durability studies on fiber reinforced EAF slag concrete for pavements. Construction and Building Materials, 163, 471-481.

Pellegrino, C., & Faleschini, F. (2013). Experimental Behavior of Reinforced Concrete Beams with Electric Arc Furnace Slag as Recycled Aggregate. ACI Materials Journal, 110(2).

Pellegrino, C., & Gaddo, V. (2009). Mechanical and durability characteristics of concrete containing EAF slag as aggregate. Cement and Concrete Composites, 31(9), 663-671.

Pellegrino, C., Cavagnis, P., Faleschini, F., & Brunelli, K. (2013). Properties of concretes with black/oxidizing electric arc furnace slag aggregate. Cement and Concrete Composites, 37, 232-240.

Pomaro, B., Gramegna, F., Cherubini, R., De Nadal, V., Salomoni, V., & Faleschini, F. (2019). Gamma-ray shielding properties of heavyweight concrete with Electric Arc Furnace slag as aggregate: an experimental and numerical study. Construction and Building Materials, 200, 188-197.

Rondi, L., Bregoli, G., Sorlini, S., Cominoli, L., Collivignarelli, C., & Plizzari, G. (2016). Concrete with EAF steel slag as aggregate: a comprehensive technical and environmental characterisation. Composites Part B: Engineering, 90, 195-202.

Santamaría, A., Faleschini, F., Vegas, I., San-José, J.-T., Pellegrino, C., González, J.J. (2017). A comparison between european electric arc furnace slags. EUROSLAG - 9th European Slag Conference. Euroslag Publication No 8. ISSN 1617-5867. Metz (Francia). 11-13Oct 2017.

Santamaría, A., Ortega-López, V., Skaf, M., Chica, J. A., & Manso, J. M. (2019). The study of properties and behavior of self compacting concrete containing Electric Arc Furnace Slag (EAFS) as aggregate. Ain Shams Engineering Journal.

SeismoSoft. SeismoStruct – a computer program for static and dynamic nonlinear analysis of frames structures; 2013. Available at: http://www.seismosoft.com.

Zanini, M. A. (2019). Structural reliability of bridges realized with reinforced concretes containing electric arc furnace slag aggregates. Engineering Structures, 188, 305-319.